

CTR Insulator Conference, Los Alamos, NM. June 1976
M...

Tritium Transport in Non-Metallic Solids

Contributors:

CONF - 760558 - 6

- C. Alexander
- R. Causey
- D. Chandra
- ✓ T. Elleman (Principal Investigator)
- J. Fowler
- A. Payne
- C. Ravenbakht
- L. Zumwalt
- K. Verghese

NOTICE
This report was prepared as an account of work sponsored by the United States Government. Neither the United States nor the United States Energy Research and Development Administration, nor any of their employees, nor any of their contractors, subcontractors, or their employees, makes any warranty, express or implied, or assumes any legal liability or responsibility for the accuracy, completeness or usefulness of any information, apparatus, product or process disclosed, or represents that its use would not infringe privately owned rights.

Introduction

Nonmetallic solids may be used in fusion reactors as tritium diffusion barriers, insulators, structural components, or protective coatings to lower plasma poisoning from first wall sputtering. The literature on hydrogen permeation, diffusion, and solubility in metals is quite extensive but little information exists on hydrogen transport or solubility in nonmetals. The purpose of the present investigation is to determine hydrogen or tritium permeabilities, diffusivities, and solubilities in nonmetallic solids of potential interest to the CTR program. A considerable amount of information has now been obtained on tritium diffusion coefficients in a variety of nonmetallic solids but the permeability and solubility studies are in an early stage.

MASTER

OT E(40-1)-4721

elb

Work supported by ERDA Contract

USAEC-AT-(40-1)-4721

Techniques and Results

I. Permeation Studies

The hydrogen permeation apparatus shown in Figure 1 has been built and leak tested. It consists of a large reservoir containing a mixture of inert gas, hydrogen and tritium which is in contact with a thin permeation specimen. Gas permeating through the disk is swept into an ionization chamber and the tritium content is monitored as a measure of the hydrogen and tritium permeating through the disk. The tritium here is used only as a tracer for the hydrogen permeating the specimen. A rapidly flowing gas blanket surrounding the sample tube is intended to minimize the transport of tritium to the ionization chamber by routes which bypass the permeation specimen. Associated systems allow sampling of the gas for tritium content, introduction of tritium through either tritiated water electrolysis or heating of irradiated ^6Li samples, and purification of the entrance gases through cold trapping and oxygen gettering.

The principal problem to date has concerned difficulties in developing a specimen bonding technique which remains leak-tight up to the planned maximum temperatures of 1300C. Efforts to employ the ceramic-metal bonding techniques involving interdiffusion of platinum metal with ceramics which have been reported by de Bruin⁽¹⁾ have not been successful. The current effort is in two directions, the use of high temperature Ti-Cr-V brazes developed by ORNL for specimen sealing⁽²⁾ and the substitution of the single-crystal permeation specimens with commercially available sintered ceramic tubes for permeation studies of sintered specimens.

Even if suitable bonding techniques are developed, it is not clear that the single-crystal permeation experiments will be successful as recent diffusion results suggest that tritium breakthrough times may be excessively long.

II. Tritium Diffusion Studies

A. Techniques

Tritium diffusion coefficients were measured by injecting tritium into specimens through neutron transmutation of a surface blanket of Li-6 fluoride or carbonate followed by measurement of the time rate of tritium release during postirradiation heating. Samples were heated in a hydrogen-helium or pure helium sweep gas which had been gettered with heated titanium and liquid

nitrogen. Released tritium was detected by an ion chamber placed downstream of the sample. Release fractions were determined after increasing sample temperatures to 1200C. at the conclusion of the run and assuming that all tritium was thereby driven from the specimens. The requirement of measurable release rates generally constrained the experiments to temperatures which produced diffusion coefficients in the range 10^{-15} cm²/sec to 10^{-9} cm²/sec. Identical temperature ranges were therefore not employed for all specimens.

Figure 2 displays a typical preheat tritium profile and the diffusion solution used to analyze results. All specimens were treated as uniform slabs unless BET surface area measurements showed a small effective particle size. An equivalent sphere model using a particle radius consistent with the surface measurements was then used to analyze results. Efforts were made to obtain specimens of known high purity, density and characterization but other less well characterized solids were also run to assess the variation in results. Table I summarizes the materials for which diffusion measurements have been made.

B. Form of Released Tritium

A fraction of the released tritium could be removed from the sweep gas by cold trapping. This condensed fraction could be extracted into an aqueous phase and was presumably tritiated water. The percent of total released tritium which could be trapped ranged from 70-80% for powdered oxide specimens to only 10-20% for single crystal specimens. Adding hydrogen to the sweep gas did not significantly alter the condensible fractions so the tritiated water must come from the specimens and not be produced through post-release exchange. Annealing specimens prior to tritium injection and storing only in inert atmospheres produced only small reductions in the condensible component. Condensation was principally observed with metal oxides but could occur with other materials. For example, essentially all of the tritium released from vapor deposited β -SiC could be removed by cold trapping. However, ultrasonic cleaning of these specimens produced a marked decrease in the condensible fraction.

Figure 3 shows the tritium diffusion coefficients measured for Al_2O_3 powders with and without cold trapping. It is apparent that the tritiated water is released at a somewhat faster rate than the non-condensable tritium as consistently higher diffusion coefficients were observed without trapping. However, the difference is not large and was even smaller in a similar study

carried out with BeO powders. Since the variation in D produced by cold trapping is similar to the uncertainty between successive measurements, no differentiation between condensible and noncondensable tritium has been made in the general determination of diffusion coefficients.

The most likely explanation for the results is that some fraction of the diffusing tritium encounters water near the surface and exchanges with the hydrogen prior to release of the water. Diffusion to the point of exchange is therefore the primary rate limiting step for the tritium release and not the release rate of the water.

C. Impurity Effects

Some differences in measured diffusion coefficients for the same material were too great to explain through accelerated diffusion along grain boundaries and presumably reflect impurity effects. One illustration is Figure 4 which plots measured diffusion coefficients for single crystal Al_2O_3 , sintered Al_2O_3 and Lucalox. The D's for sintered Al_2O_3 are somewhat above those for the single crystal material which is consistent with rapid tritium movement along incoherent grain boundaries or pores in the sintered solid. However the D's for Lucalox (99.8% Al_2O_3 , 0.2% MgO) are approximately four orders of magnitude higher than the values for undoped Al_2O_3 . This effect is not explainable in terms of grain boundary effects since the nominal Lucalox grain size of 30 μm was roughly 1.5 times the recoil range of the tritium atoms. Kitazawa and Coble⁽³⁾ have observed a similar increase in defect diffusion rates for MgO-doped versus undoped Al_2O_3 and a number of examples of impurity accelerated diffusion occur in the literature for ceramics⁽⁴⁻⁷⁾.

A second example appears in Figure 5 where higher tritium diffusion coefficients are observed for Al-doped, hot-pressed, and single-crystal SiC than with undoped material. Again, grain boundary effects cannot explain the disparity since single-crystal specimens comprise one set of the higher data. It is conceivable that the lower set of points are anomalous and the tritium diffusion is controlled by unrecognized trapping effects. This seems unlikely since the release curves were classical and showed no evidence of tritium trapping.

D. Surface Absorption Effects

Most tritium release curves were classical and gave values of D

consistent with single values for the diffusion activation energy. Release rates were unaffected by hydrogen concentrations in the flow gas so the calculated values of D are believed to represent diffusion controlled release from the specimens. Table II summarizes the measured values for the expression:

$$D = D_0 e^{-Q/RT}$$

for all specimens studies to date which behaved classically. Also included are the standard deviations and temperature ranges for each material. Boron carbide was included as a material of study principally because of the potential interest in transmutation induced tritium diffusion in B_4C reactor control rods rather than as a result of any anticipated use in fusion reactors.

One material, pyrolytic carbon, did exhibit release behavior which appears to reflect absorption controlled rather than diffusion controlled processes. Samples of LTI pyrolytic carbon which were similar to the coatings used on HFGR reactor fuels were obtained on inert ZrO_2 substrates from General Atomics Co. Tritium release rates from these specimens increased when hydrogen was added to the flow gas to give widely different apparent diffusion coefficients for a hydrogen free and a high-hydrogen sweep gas (Figure 6). It was further observed from the tritium concentration profiles within the specimens that all of the released tritium was coming from the top 25 μm of the specimen with very little migration of the deeper tritium. The profiles were determined by chemically removing layers from annealed specimens and measuring the tritium within each layer. Open pore structure in LTI coatings is reported in the literature⁽⁸⁾ so it seems likely that the high release rate produced by hydrogen sweep gas was a consequence of accelerated tritium exchange on pore surfaces rather than a bulk process. This interpretation is supported by experiments in which pyrolytic carbon specimens were exposed to gaseous tritium and then sectioned. The tritium was observed to penetrate only 25 μm into the specimens.

Laminar specimens of pyrolytic carbon produced markedly lower apparent diffusion coefficients which were unaffected by hydrogen in the sweep gas. Values of D inferred from profile measurements were consistent with the values obtained from release experiments. These values are therefore tentatively considered as diffusion coefficients and are included in Table II. It is recognized, however, that a material as complex as pyrolytic carbon

could exhibit strikingly different transport properties with different morphologies and to even interpret results in terms of diffusion processes may be inappropriate.

It is of interest to note that tritium diffusion coefficients determined from silicon-doped pyrolytic carbon correspond almost exactly with the values for vapor deposited SiC rather than the lower undoped pyrolytic carbon (Figure 7). Electron-microprobe scans were run to determine if high Si concentrations existed near the surface but only uniform distributions were observed. No explanation is offered for this possibly coincidental agreement between Si-doped pyrolytic carbon and SiC.

III. Solubility Studies

Experiments are being carried out to estimate hydrogen solubilities in ceramics. In the event that permeation values prove difficult to obtain experimentally, the product of diffusivity and solubility will provide an estimate of permeability where grain boundary effects are neglected.

From the known diffusion coefficients, the time required for the equilibration of a solid of known dimensions with an external hydrogen blanket can be calculated. Specimens of alumina have been equilibrated in flowing deuterium-argon streams at elevated temperatures for time periods longer than the calculated equilibration times. The specimens have then been heated in a vacuum furnace attached to a residual gas analyzer on a preprogrammed isochronal annealing temperature schedule. Weighed TiD_2 powders have been used as standards to relate the RGA signal to released deuterium. Only preliminary results have been obtained to date but they suggest that hydrogen solubilities in Al_2O_3 are quite low.

IV. Ion Implantation Studies

The appearance of condensable tritium in the flow gas may reflect hot atom reactions which result from the energetic introduction of tritium into the specimens. Specimens of single crystal Al_2O_3 are being irradiated with 2 MeV deuterons in the campus van de Graaff accelerator to particle fluences in excess of those employed in the tritium injection experiments. The specimens will then be heated and the mass distribution of released deuterium determined with the RGA. These experiments will hopefully identify the chemical species containing the injected deuterium which are released during

heating. A comparison of the release spectra for injected specimens with those simply heated in flowing deuterium should help clarify if hot atom reactions are involved in the formation of condensible compounds.

Discussion

The previous work on hydrogen diffusion in nonmetallics is so meager that few comparisons with previous work can be made. Roberts and Roberts⁽⁹⁾ reported data for hydrogen diffusion in single crystal α -Al₂O₃ which fall about an order of magnitude below the present results when extrapolated from the 1400-1630C. range of measurement. This agreement appears satisfactory considering the extrapolation involved.

Scott and Wassell⁽¹⁰⁾ studied tritium release from irradiated BeO single crystals. Their activation energy and diffusion coefficients are in substantial agreement with the present work. They also observed that some tritium was released from BeO powders as water vapor which is in agreement with the present work on BeO powders.

A number of measurements of hydrogen diffusion in glasses have been made which typically exhibit activation energies of 8-13 kcal/mole⁽¹¹⁾, well below the 30.2 kcal/mole observed for SCB glass. However, the more highly doped glasses typically have higher activation energies. Matzke has observed activation energies of 42-52 kcal/mole for tritium diffusion in ion-injected glasses.⁽¹²⁾ The SCB glass in the present study was originally developed as a hydrogen barrier for SNAP ZrH reactors. A permeation activation energy of 30 kcal/mole was measured by Al⁽¹³⁾ which agrees well with the diffusion activation energy. Since hydrogen solubility in glasses is not a strong function of temperature, permeation and diffusion activation energies could be similar.

No information has been found on hydrogen transport in other materials employed in the present study.

Tritium diffusion coefficients and activation energies for the materials studied are quite different from the values associated with hydrogen diffusion in metals. At a reference temperature of 600C, the D's associated with refractory metals are typically 6-10 orders of magnitude larger than the D's measured here. Diffusion activation energies for hydrogen in metals are typically 9-15 kcal/mole in contrast to 30-64 kcal/mole for ceramics. These disparities suggest that tritium diffusion in ceramics is more complex than in metals and that hydrogen bonding effects and even compound formation, molecular diffusion, or complex defect migration may play a role in hydrogen transport in nonmetallics.

The low measured diffusion coefficients for nonmetallics suggest that they may be effective tritium barriers in CTR systems. The equilibrium

transport of any diffusing species through successive layers of homogeneous materials is usually complicated by effects at the interfaces; however, within a given region the concentration gradient is uniform and known from a straightforward application of Fick's first law. If we assume that a tritium diffusion barrier consists of a thin layer of ceramic bonded to a metal substrate, a simple expression for the equilibrium permeation rate with the coating to the rate without the coating can be obtained if the tritium concentration is assumed to be uniform across the interface and zero at the exit face. Figure 8 illustrates this condition and gives values for the ratio of permeation rates for an assumed coating thickness of 0.1 mm, a substrate thickness of 2 mm, and a temperature of 600C. The metal diffusion coefficients were selected from the review paper by Stickney⁽¹⁴⁾ while the coating diffusion coefficients were taken from Table II. It is apparent that all coatings produce a pronounced decrease in the equilibrium permeation rate which ranges from 2 orders of magnitude to 17 orders of magnitude. The coatings divide into three general groups with pyrolytic carbon as the most effective; Al_2O_3 , B_2O_3 , and SiC in the next group; and Y_2O_3 , Lucalox, Yttralox and SCB glass as the least effective barriers.

This simple model neglects any accelerated diffusion between grains which could greatly increase permeation rates in real coatings. It further neglects interface partition effects which would likely increase the effectiveness of coatings. The model does indicate that nonmetallics have the potential for being effective tritium barriers if suitable methods can be devised for applying coatings and for minimizing grain boundary transport effects.

Conclusion

The low tritium diffusion coefficients in nonmetallic solids suggest that they may prove to be effective tritium barriers in CTR systems. Tritium or hydrogen permeation studies of coated specimens fabricated by various available techniques would appear to be desirable.

References

1. De Bruin, H., A. F. Moodie and C. E. Warble, J. Mat. Sci. 7:909-18 (1972).
2. Canonico, D. A., N. C. Cole and G. M. Slaughter, ORNL/TM-5195 (1976).
3. Kitazawa, K. and R. L. Coble, J. Am. Ceram. Soc. 57:250-3 (1974).
4. Mokhov, E. N., S. K. Koprov and Y. A. Vodakov, Sov. Phys. SS. 13-3120-2 (1972).
5. Johnson, O. W., S. H. Paek, and J. W. De Ford, J. Appl. Phys. 46:1026-33 (1975).
6. Austerman, S. B., J. Nucl. Mat. 14:248-57 (1964).
7. Yamaguchi, G., M. Nakano, and M. Tosaki, Bull. Chem. Soc. Japan 42:2801-7 (1969).
8. Kaae, J. L., Carbon 13:55 (1975).
9. Roberts, E. W. and J. P. Roberts, Bull. Soc. Fr. Ceram. II:3 (1967)
10. Scott, K. T. and L. L. Wassell, Proc. Brit. Ceram. Soc., I:375 (1967).
11. Doremus, R., Glass Science, John Wiley, New York (1973) Chap. 8
12. Matzke, HJ, Z. Naturforschg. 22a 965 (1967).
13. J. Walter, Personal communication, Atomics International.
14. Stickney, R. E., From The Chemistry of Fusion Technology, Plenum Press (1972).

Table I - SPECIMEN PROPERTIES AND SUPPLIERS

<u>Material</u>	<u>Composition</u>	<u>Supplier</u>
Lucalox	Al ₂ O ₃ (99.8%), MgO (0.2%), Si (trace)	General Electric
BeO Sint.	Mg (0.2%), Si (0.32%), BET area 0.11 m ² /g.	Brush Wellman
BeO (S.C.) ⁽²⁾	Impurities <.05% ⁽¹⁾	Rockwell Int.
SiC (S.C.) ⁽²⁾ Al-doped	Al (0.6%)	Carborundum
α-SiC ⁽²⁾	Al (50 ppm) trace 0	Carborundum
β-SiC ⁽²⁾	Impurities <.05% ⁽¹⁾	R. Davis - NCSU
Yttralox	Y ₂ O ₃ (89%), ThO ₂ (10%), Nd ₂ O ₃ (1%)	General Electric
SCB Glass	SiO ₂ (46.1%), BaO (31.3%), Al ₂ O ₃ (8.3%) TiO ₂ (12.5%), Cr ₂ O ₃ (1.0%), Eu ₂ O ₃ (0.8%)	Atomics Int.
Y ₂ O ₃	Y ₂ O ₃ (99.99%)	Ceradyne
SiC - Al-Doped (Hot-Pressed)	Al (2.0%), Fe (0.3%)	Norton
PyC Lam.	----	General Atomic
Si-Doped PyC	Si (40 w/o)	General Atomic
B ₄ C	----	Manford Devel. Lab.
Al ₂ O ₃ (S.C.) ⁽²⁾	----	Linde Corp.

(1) Impurity levels determined by microprobe analyses

(2)(S.C.) = Single Crystal

Table II: Summary of Measured Diffusion Coefficients

Material (S. C. - single crystal)	Number of points	D_0 (cm^2/sec)	D_0^+ (cm^2/sec)	D_0^- (cm^2/sec)	Q (kcal/mole)	σ (Q) (kcal/mole)	Temperature range ($^{\circ}\text{C}$)
Al_2O_3 S.C.	9	3.26	9.86	1.08	57.2	2.4	600-1000
Al_2O_3 sintered	7	7.35×10^{-2}	0.247	2.19×10^{-2}	43.8	2.5	600-900
BeO S.C.	14	1.11×10^{-2}	8.91×10^{-2}	1.39×10^{-3}	52.5	4.7	650-1200
BeO sintered	11	7.00×10^{-2}	0.445	1.10×10^{-2}	48.5	3.6	500-950
Lucalox	15	39.8	357	4.43	41.8	3.2	360-570
α - SiC S.C.	12	1.09×10^{-2}	2.92×10^{-2}	4.05×10^{-3}	54.9	2.5	700-1300
β - SiC S.C.	10	28.4	172	4.55	65.0	4.1	750-1000
Al-doped α - SiC S.C.	8	4.04×10^{-4}	3.80×10^{-3}	4.29×10^{-5}	34.0	4.2	450-950
Al-doped hot- pressed α - SiC	11	0.904	6.68	0.147	48.2	3.5	500-800
SCB glass	10	2.95×10^{-4}	6.34×10^{-4}	1.37×10^{-4}	30.2	1.2	350-800
Y_2O_3 hot-pressed	8	0.431	7.13	2.6×10^{-2}	39.1	4.3	420-620
Yttralox	6	3.87	32.2	0.464	39.5	3.1	350-600
Laminar pyrolytic Carbon	10	3.3×10^2	2.0×10^3	54	98.4	5.7	1100-1450
β - Vapor deposited SiC	8	1.6	3.4	0.7	73.6	2.0	800-1300
Si-doped pyrolytic Carbon	13	1.1×10^{-3}	3.9×10^{-3}	3.1×10^{-4}	53.6	3.6	900-1400
Boron Carbide	14	1.1×10^{-6}	3.3×10^{-6}	3.9×10^{-7}	16.8	1.6	300-700

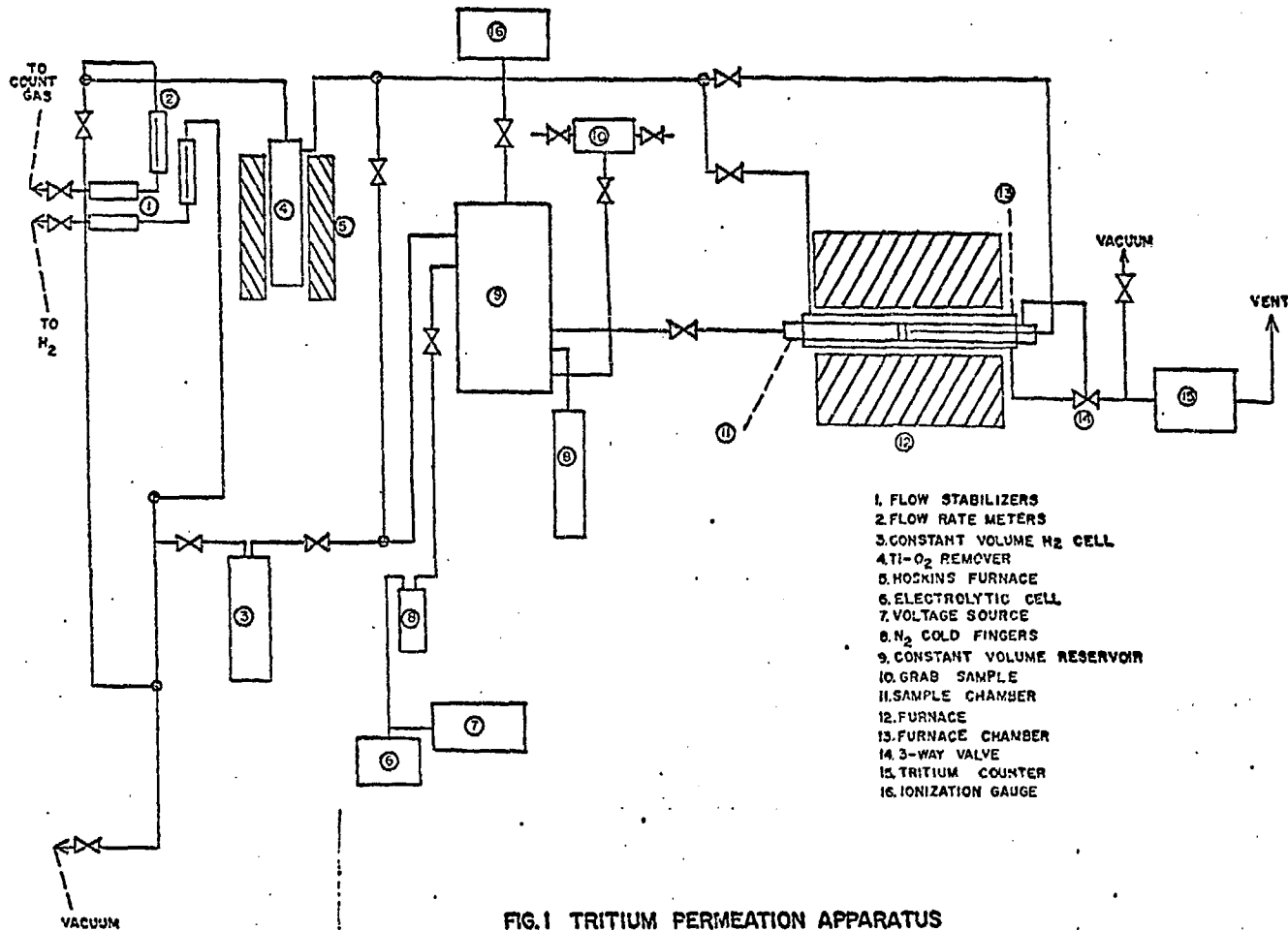
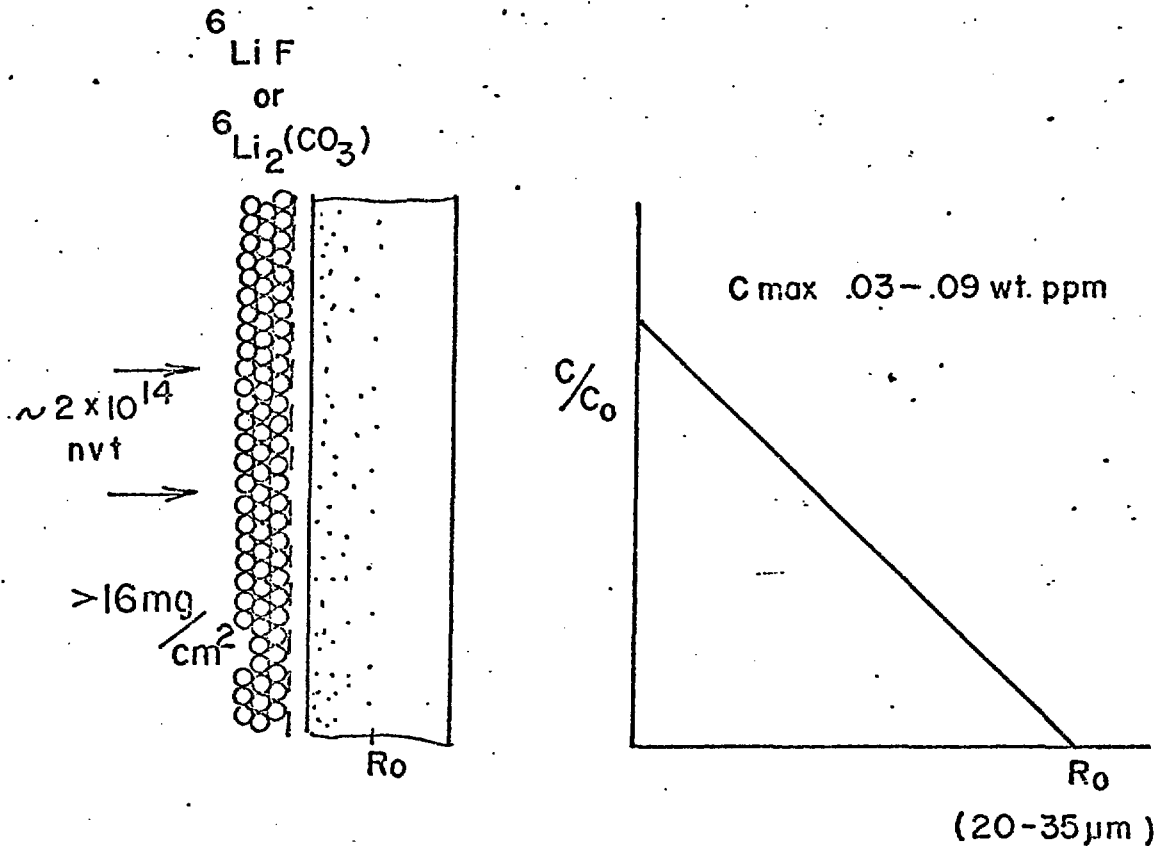


Figure 2 TRITIUM INJECTION METHOD



SHORT-TIME DIFFUSION SOLUTION

$$f(t) = \frac{4}{R_0} \sqrt{\frac{Dt}{\pi}}$$

$f(t)$ = fraction released

R_0 = range

D = diffusion solution

t = heating time

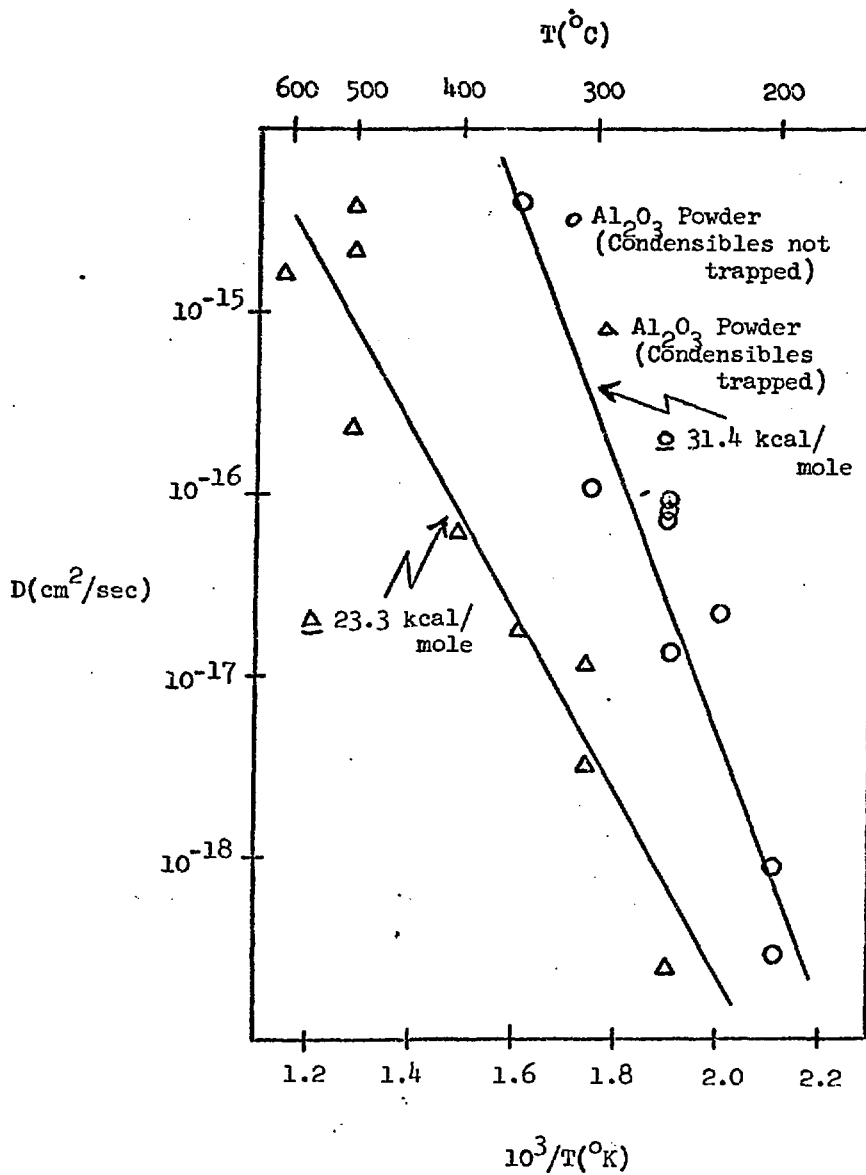


Figure 3. Arrhenius plot for tritium diffusion in alumina (Al_2O_3)

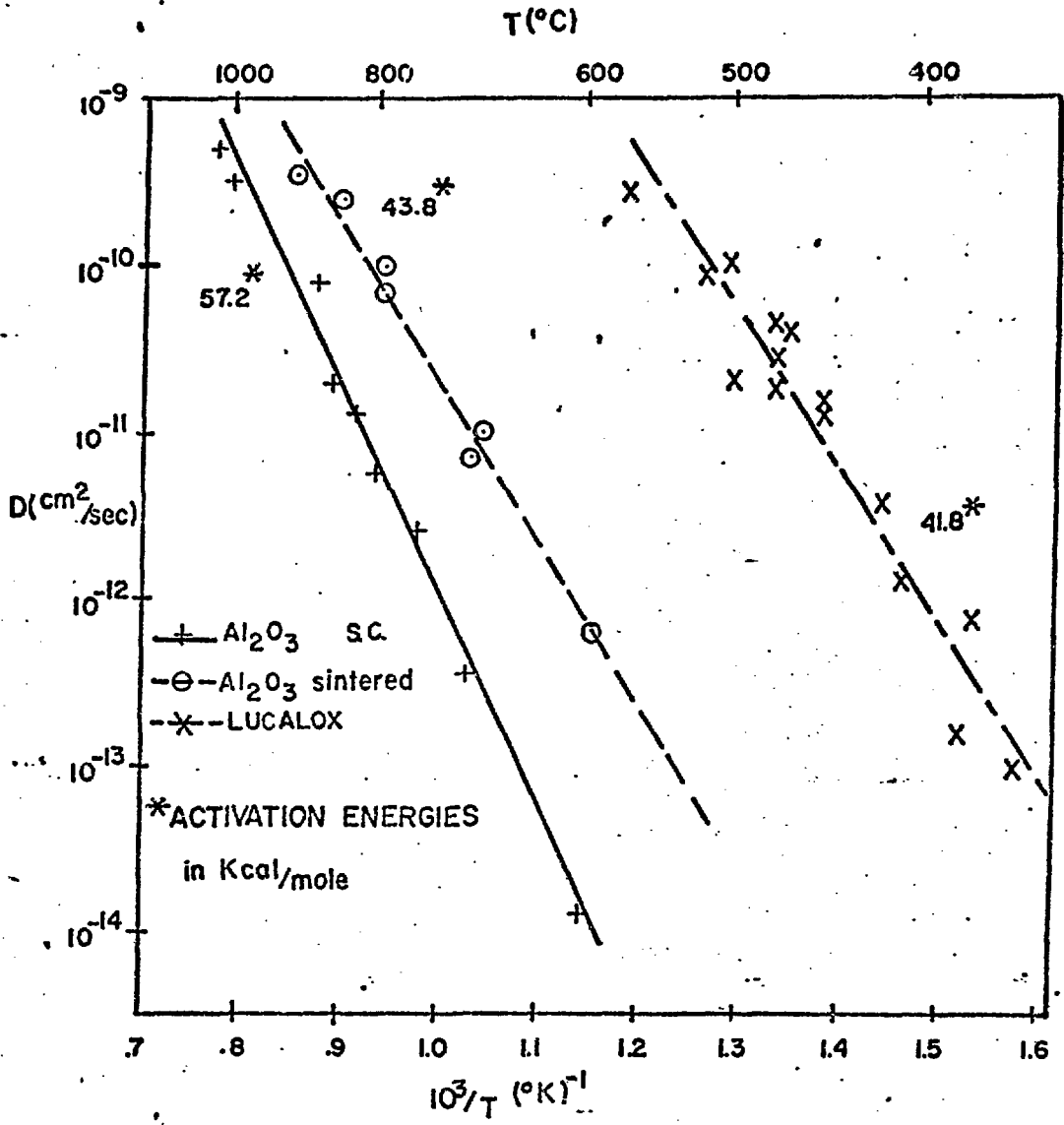


Figure 4. Arrhenius plot for tritium diffusion in single crystal and sintered alumina and Lucalox.

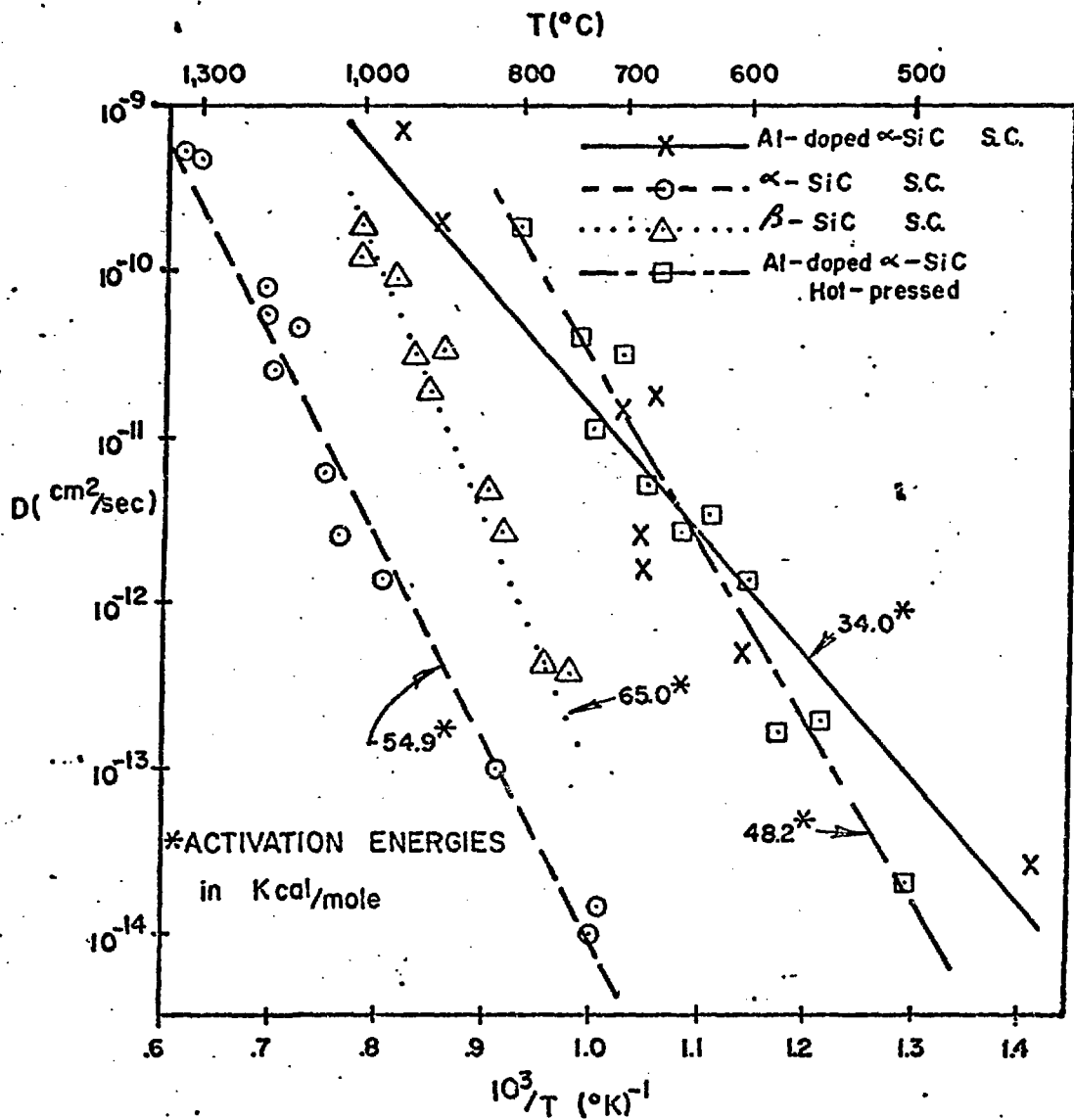


Figure 5. Arrhenius plot for tritium diffusion in α and β -silicon carbide single crystals, aluminum-doped single crystal α -silicon carbide, and aluminum-doped hot-pressed α -silicon carbide.

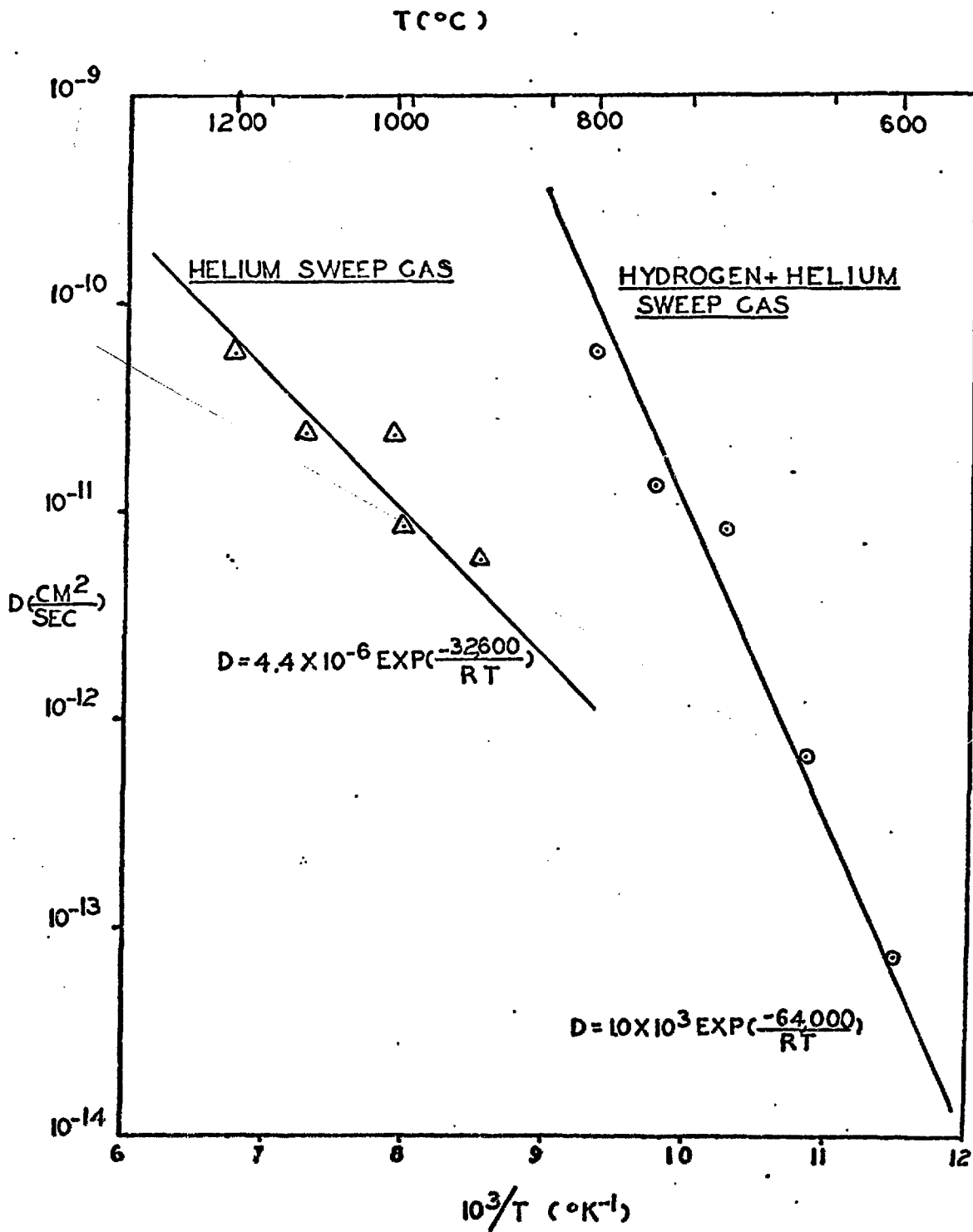


Figure 6 - Tritium Diffusion Coefficients in Pyrolytic Carbon

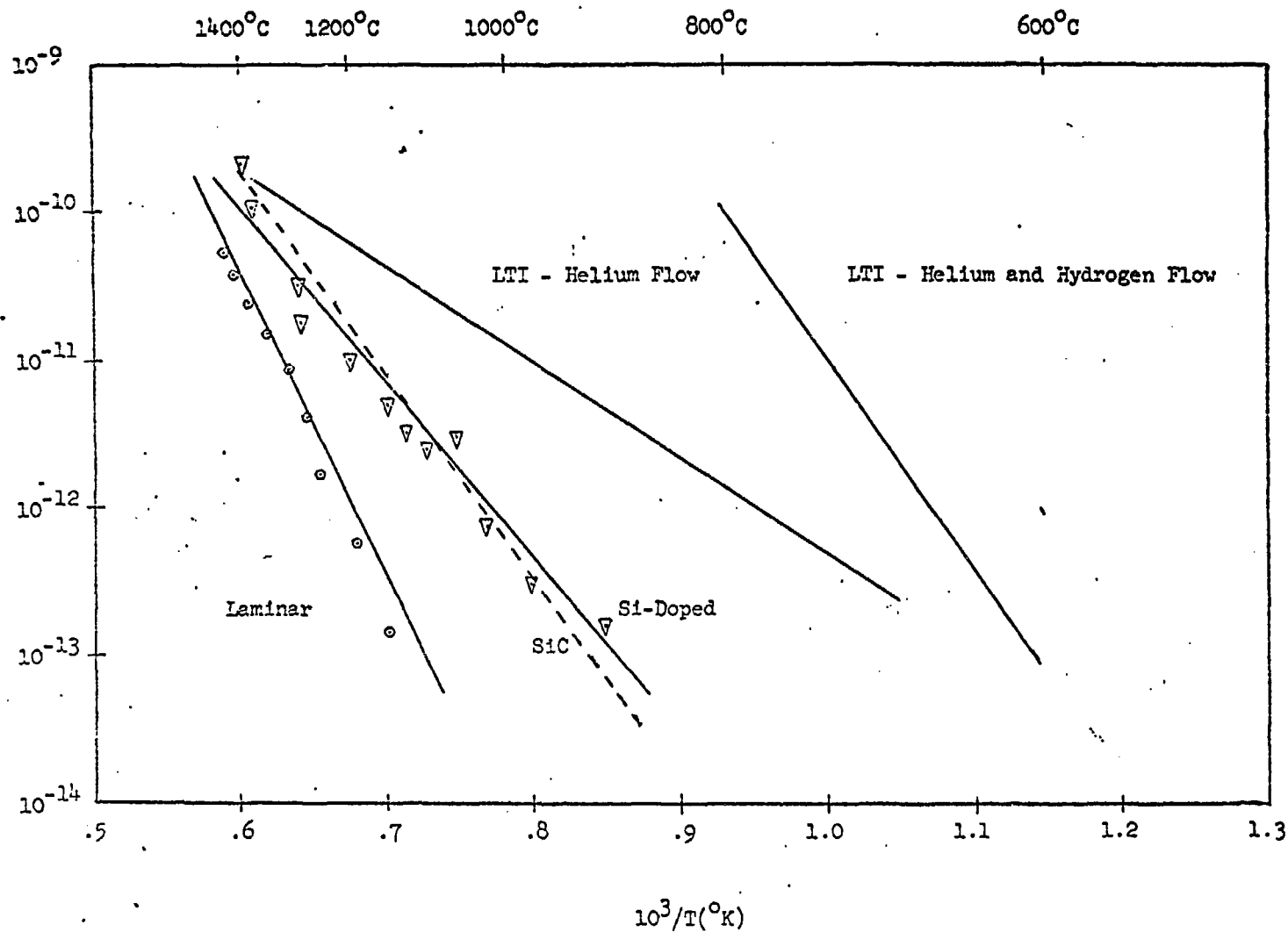
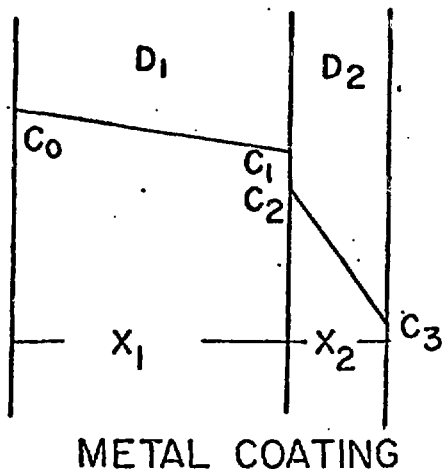


Figure 7 - TRITIUM DIFFUSION IN PYROLYTIC CARBON

Figure 8 - Equilibrium Tritium Transport Through Non-Metallic Coatings



IF:

$$C_1 = C_2$$

$$C_3 = 0$$

SYSTEM AT
EQUILIBRIUM

THEN:

$$\frac{R'}{R} = \frac{\text{EQ. RELEASE RATE - COATING}}{\text{EQ. RELEASE RATE - NO COATING}} = \frac{\left(\frac{X_1}{D_1}\right)}{\left(\frac{X_2}{D_2}\right) + \left(\frac{X_1}{D_1}\right)}$$

FOR $T = 600\text{ C}$ $X_1 = 0.2\text{ cm}$ $X_2 = .01\text{ cm}$.

$$\left(-\log \frac{R'}{R}\right)$$

<u>COATINGS</u>	<u>W</u>	<u>Mo</u>	<u>Nb</u>	<u>S.S. (Aust.)</u>
Al_2O_3	6-8	6-7	7-8	6-7
BeO	7-9	7-9	8-10	7-9
Y_2O_3	4	4	5	4
Si C	6-10	6-9	7-10	6-9
LUCALOX	3	2	3	2
YTTRALOX	3	3	4	3
SCB GLASS	5	5	6	5
Py C (LAM.)	16	16	17	16